Base Pressure of a Projectile Within the Transonic Flight Regime

W. L. Chow*
University of Illinois at Urbana-Champaign, Urbana, Illinois

An equivalent body concept is developed to examine the base pressure problem of a transonic flow past a blunt-based projectile. The inviscid flow is established by finite difference computations of the axisymmetric potential equation. All viscous flow processes are treated through integral formulations. The strong viscid-inviscid interaction is clearly illustrated from the method of approach to the problem. A definition of the base pressure that is compatible with that for the supersonic flow regime has been developed for the transonic flow regime. An analysis of the asymptotic far-wake condition relates a needed parameter to the total drag experienced by the projectile. Results are obtained for transonic (both subsonic and supersonic) approaching flow conditions and are also compared with the available experimental data. Extension to cases with small angles of incidence is also discussed.

Nomenclature

$A_i, B_i, \ldots, G_i$ = coefficient functions
D_t, C_{Dt} = total drag force, total drag coefficient of the projectile
h_b = height of reverse flow
P = pressure
R_b = equivalent body radius for inviscid flow analysis
R_d = radial coordinate of the dividing streamline
R_e = radial location of the edge of the viscous layer
R_0 = base radius of the projectile
s = velocity slope parameter for the recompression region [see Eq. (4a)]
u, v = velocity component in z, r coordinate system
x = z coordinates for the jet mixing process whose origin is located at the base
z, r = cylindrical coordinates
z_R = z location where the equivalent body radius reaches δ^*_{asy}
δ^* = displacement thickness of the shear layer
δ_a = thickness of the viscous layer above the dividing streamline in the mixing and recompression regions, $= R_e - R_d$
δ_b = thickness of the forward-flowing viscous layer below the dividing streamline in the mixing and recompression regions, $R_d - h_b$
δ_e = thickness of viscous layer in the redevelopment region
ϵ = eddy diffusivity along the dividing streamline
ζ_a = dimensionless radial coordinate for the shear layer above the dividing streamline, $(r - R_d)/\delta_a$
ζ_b = dimensional radial coordinate for the reverse flow region, r/h_b
ζ_ℓ = dimensional radial coordinate for the forward flowing shear layer below the dividing streamline, $(r - R_d + \delta_b)/\delta_b$
ρ = density
τ = shear stress
ϕ = dimensionless velocity, u/u_e

Subscripts

asy = far-wake condition
b = reverse flow
cyl = cylinder
d = dividing streamline
e = edge of the viscous layer
G = projectile base (see Fig. 2)
m = end of the mixing region (also, beginning of recompression region)
og = ogive
R = point of reattachment
w = wake flow in the region of flow redevelopment
∞ = approaching flow condition

Received Nov. 14, 1983; presented as Paper 84-0230 at the AIAA 22nd Aerospace Sciences Meeting, Reno, Nev., Jan. 9-12, 1984; revision received March 26, 1984.

*Professor of Mechanical Engineering, Department of Mechanical and Industrial Engineering. Associate Fellow AIAA.

Introduction

DESPITE the prevailing popularity of solving fluid dynamic problems through large-scale numerical computations of the Navier-Stokes equation, study of the base pressure problem from the conventional approach provides a unique opportunity to illustrate vividly the flow mechanisms governing the phenomenon of these problems. It is well known that the viscous flow plays a role as important as the external inviscid flow in the establishment of the overall flow pattern. This feature has been classified as a strong viscid-inviscid interaction. Since the viscous flow is always located along the edge of the inviscid flow region, the viscous flow is thus guided by the inviscid flow in the sense of the boundary-layer concept. On the other hand, in direct association with the inviscid flowfield, the geometry of the wake as well as the pressure level and distribution within the wake are dependent upon the viscous flow processes of jet mixing, recompression, reattachment, and redevelopment behind the base. This mutual dependency between the inviscid and viscous flows was pointed out by Crocco and Lees.[1] Much work on base pressure has been carried out since that time.[2-16] It should be noted that all of these investigations were restricted to problems with supersonic external streams. Other than the limited few exceptions,[15,16] none of these analyses considered the process of redevelopment after reattachment.

In a more detailed examination of the recompression-reattachment process of a turbulent free shear layer,[14] it was learned that this same integral analysis can be applied to study the base pressure problems in any other flow regime. An examination of base pressure problems of incompressible wedge flow was later carried out.[17-19] The elliptic inviscid flow is established from conformal mapping. The viscous flow was guided by the established inviscid flow, while the characteristic parameters describing the inviscid flow were determined from viscous flow processes. This analysis also led to the study of the base pressure problem for the transonic flow past a backward-facing step in the two-dimensional and axisymmetric configurations.[20-23] Indeed, since the pressure field is established from the inviscid flow, it would be appropriate to simulate the pressure field on the basis of an "equivalent body." The solution of the transonic inviscid flow was established from the finite difference computations of the potential equation. It was learned that the point of reattachment behaved as a saddle-point singularity of the system of equations describing the isoenergetic viscous flow recompression. Furthermore, the pressure at the step cannot be taken as the base pressure within the transonic flow regime. It is obvious that the step pressure coefficient increases toward zero as the freestream Mach number increases toward unity; meanwhile, the base pressure coefficient decreases toward more negative values. It was also learned that studies carried out up to this point constituted only the first approximation to the problem since the resulting equivalent body established from the viscous flow analysis was not yet compatible with the equivalent body selected to establish the inviscid flow.

Additional studies have been carried out on the transonic base pressure problem. Specifically the base pressure of a six-caliber secant-ogive-cylinder projectile immersed in a transonic flow has been examined. The flow condition on the forebody, including the attached turbulent boundary together with the processes of mixing, recompression, reattachment, and redevelopment behind the base, must be included in the considerations. It will be shown that the equivalent body for this problem can be described with two characteristic parameters. It will also be demonstrated that the point of reattachment is a saddle-point singularity for the system of equations describing the viscous flow recompression. Continued computation after reattachment will reveal that the fully developed wake flow state is also a saddle-point singularity of the system of equations describing the viscous flow redevelopment. However, with additional analysis of the asymptotic state of fully developed flow, one parameter can be directly related to the total drag of the body, and the problem can be reduced to a problem of Reynolds number matching from the analysis of recompression. Extension to the case of flow with a small angle of attack will also be suggested and discussed.

Analytical Considerations

For external flow past a body, the surface pressure distribution is the item of utmost concern which supplies the basic information for the lift-drag calculations. Inasmuch as the boundary-layer concept is applicable, the pressure distribution is determined entirely from the inviscid flow geometry. For the present problem of flow past a projectile, the equivalent body geometry must be established before any viscous flow processes can be examined and studied.

The Equivalent Body

For transonic flow past a projectile, whose typical configuration is shown in Fig. 1, it is expected that after the flow separates from the base, usually a turbulent jet mixing process occurs along the wake boundary. The dividing streamline is thus energized, preparing itself for the subsequent recompression and reattachment at the end of the near wake. After reattachment, additional compression of the shear layer occurs in the early part of the redevelopment before the pressure field decays toward that of the freestream. Based on the displacement concept of the boundary layer, the equivalent inviscid body boundary would be located away from the viscous dividing streamline by a distance of the displacement thickness δ^* of the viscous layer above the dividing streamline. This reasoning leads to the specification of the equivalent body $R_b(z)$ for the present problem by

$$R_b(z) = 0 \qquad \text{for } z \le 0 \tag{1a}$$

$$= R_{og} + \delta^*(z) \qquad \text{for } 0 \le z \le z_T \tag{1b}$$

$$= R_{cyl} + \delta^*(z) \qquad \text{for } z_T \le z \le z_G \tag{1c}$$

$$= \delta^*_{asy} + (R_{cyl} + \delta^*_b - \delta^*_{asy}) e^{(-\Delta^2/1-\Delta)} \qquad \text{for } z_G \le z \le z_R \tag{1d}$$

where $\Delta = (z - z_G)/(z_R - z_G)$,

$$R_b(z) = \delta^*_{asy} \qquad \text{for } z_R \le z \tag{1e}$$

The schematic sketch of the equivalent body of projectile is shown in Fig. 2. It will be recognized that the parameters characterizing the equivalent body geometry are z_R and δ^*_{asy} for this specific projectile. It is also worthwhile to note that Δ varies from zero to unity when z is between points G and R and the second power employed in Eq. (1d) assures the slope continuity of the profile at the base. Futhermore, it can be shown that under the far-wake condition, the displacement thickness of the viscous layer approaches a finite value even when the viscous layer thickness approaches infinity at far downstream locations.

The Inviscid Flowfield

Once the equivalent body is specified for a transonic approach flow Mach number, the inviscid flow is established from relaxative finite difference calculations of the full potential equation. In fact, it follows precisely a procedure described in the study of transonic flow past a boattailed afterbody.[24,25] That procedure is discussed briefly herein. At first, a transformation is introduced to transform the infinite physical region of concern into a finite region of computation. A specific finite difference form of the transformed potential equation is written which depends upon whether the flow is locally supersonic or subsonic. A row of grid points is added below the body surface so that the tangent flow condition on the surface can be obeyed. When the finite difference equations are written for all grid points at a certain streamwise location, a tridiagonal system of equations is obtained. Values of the potential function are found by solving the system of equations. This new information is immediately employed to update the corresponding value of the grid below the body surface in satisfying the local boundary condition. This procedure is then repeated for the next streamwise location. This line-by-line sweeping of the computational plane from upstream toward downstream directions is carried out until the change in the value of the potential function is less than an arbitrarily small number for all grid points throughout the domain of computation. A convergent solution of the potential function is obtained. In the midst of computations of the potential function, the turbulent boundary-layer growth with the prevalent pressure gradient on the body surface has also been estimated from an integral approach. The equivalent body geometry is correspondingly modified to account for the displacement effect of this turbulent boundary-layer growth. Thus the boundary-layer, momentum, and displacement thicknesses of the viscous layer at the base are known as soon as the inviscid flowfield is established.

Turbulent Jet Mixing, Recompression, and Reattachment

The integral analysis of these flow processes precisely follows the early study of a flow past a backward-facing step.[23] Only a brief description of these considerations is given here. Again, an isoenergetic flow condition is assumed throughout all viscous flow regions.

Immediately behind the base, a turbulent jet mixing process occurs along the jet boundary. As one will observe later, the pressure also decreases significantly along the path of mixing in the transonic regime. Nevertheless, the mixing process can be treated on the basis of a quasi-constant pressure analysis.[26] At each location, the velocity profile is derived from a local constant pressure calculation with the same initial boundary-layer profile. A linear velocity profile with the local slope given by

$$\frac{\partial u}{\partial r} = \frac{\sigma u_e}{\pi^{1/2} x} \tag{2a}$$

is assumed, which is the inflection-point slope of an error-function mixing profile. The eddy diffusivity ϵ for this region is given by

$$\epsilon = (1/4\sigma^2) x u_e \tag{2b}$$

where x is the distance along the path of mixing measured from the origin of mixing, u_e the local freestream velocity, and σ, the spread-rate parameter for the turbulent mixing process, assumes the value of 12 throughout this series of study. The turbulent boundary layer at the step provides the initial condition. The dividing streamline velocity, the shear layer thicknesses above and below the dividing streamline, as well as the shear stress along the dividing streamline can be determined at each section along the mixing region. This mixing analysis is carried out until the section of lowest pressure along the wake is reached. The flow properties here also provide the initial conditions for the subsequent recompression process.

Prior to consideration of recompression, an average base pressure can be determined from the momentum principle. One observes from Fig. 3 that the momentum principle, when applied between the base and section m, the end of the mixing region, readily yields

$$p_b \pi R_0^2 = \int_{R_{dm}}^{R_0} P_d 2\pi r \mathrm{d}r + \pi R_{dm}^2 P_m - \int_0^{\ell_m} \tau_d 2\pi r \mathrm{d}z + \int_0^{\delta_b} 2\pi r \rho u^2 \mathrm{d}r + \int_0^{h_b} 2\pi r \rho u^2 \mathrm{d}r \tag{3}$$

where the forward flow momentum is evaluated from the linear mixing profile and the backward flow momentum is evaluated from the reverse flow velocity profile for the following recompression process. An average base pressure ratio, P_b/P_∞, may be solved from the above equation. In supersonic external flows, there is practically no pressure variation prior to recompression. Under this condition, the shear stress integral in Eq. (3) balances with the forward flow momentum, and the backward flow momentum is usually negligible. Thus, the base pressure from Eq. (3) would be equal to the uniform pressure prevailing within the wake for the supersonic flow condition. In transonic flow, the pressure variation immediately behind the base is so severe that the above expression is needed to give a more realistic estimation of the average base pressure and base drag.

Recompression essentially follows that which has been developed previously.[23] At each section the dimensionless velocity of the flow has a profile of

$$\phi = u/u_e = \phi_d + s\zeta_a + (3(1-\phi_d) - 2s)\zeta_a^2 + [s - 2(1-\phi_d)]\zeta_a^3 \quad 0 \le \zeta_a \le 1 \tag{4a}$$

above the dividing streamline, a linear profile of

$$\phi = u/u_e = \phi_d \zeta_\ell \qquad 0 \le \zeta_\ell \le 1 \tag{4b}$$

below the dividing streamline for the forward wake flow, and a cosine profile of

$$\phi = u/u_e = -\phi_b \cos(\pi/2)\zeta_b \quad 0 \le \zeta_b \le 1 \tag{4c}$$

for the reverse wake flow, where

$$\phi_d = \frac{u_d}{u_e}, \quad \phi_b = \frac{u_b}{u_e}, \quad \zeta_a = \frac{r - R_d}{\delta_a}, \quad \zeta_\ell = \frac{r - R_d + \delta_b}{\delta_b}$$
$$\zeta_b = \frac{r}{h_b}, \quad \delta_a = R_e - R_d, \quad \delta_b = R_d - h_b \tag{4d}$$

The slope parameter s in Eq. (4a) is linearly coupled to ϕ_d, and the proportional constant is evaluated at the initial section of the recompression region. This manipulation assures the fact that both ϕ_d and s vanish together at the section of reattachment. A locally triangular geometry is also assumed for the wake flow so that the wake centerline which divides the forward and reverse flow also shall pass through the point of reattachment as it should.

A system of five ordinary differential equations is obtained to describe the process of recompression. They are given by

$$A_i \frac{\mathrm{d}R_e}{\mathrm{d}z} + B_i \frac{\mathrm{d}R_d}{\mathrm{d}z} + C_i \frac{\mathrm{d}\phi_d}{\mathrm{d}z} + D_i \frac{\mathrm{d}h_b}{\mathrm{d}z} + E_i \frac{\mathrm{d}\phi_b}{\mathrm{d}z} = F_i \frac{\mathrm{d}C_e}{\mathrm{d}z} + G_i \qquad i = 1,\ldots,5 \tag{5}$$

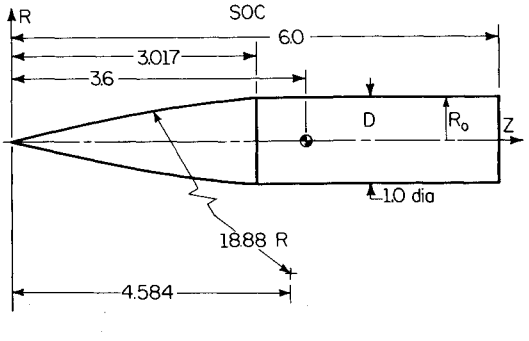

Fig. 1 A six-caliber secant-ogive-cylinder projectile.

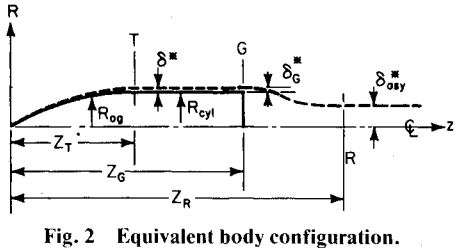

Fig. 2 Equivalent body configuration.

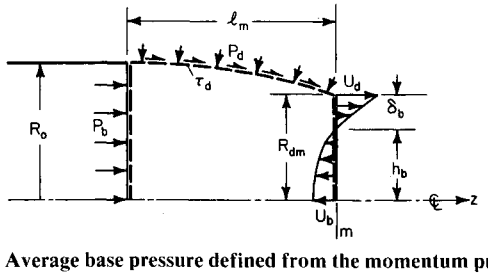

Fig. 3 Average base pressure defined from the momentum principle.

The first two equations are obtained from the continuity principle for the viscous layers above and below the dividing streamline, respectively. The next two were the momentum relations for the two layers, and the last was derived from the condition of local triangular wake geometry. Coefficients A_i, $B_i,\ldots,G_i$ (see Ref. 23 for expressions of these functions) are complicated functions of flow properties and conditions. Equation (5) describes the variation of the locations of the edge of shear layer R_e, the dividing streamline R_d, and its velocity u_d, together with the reverse flow height h_b and velocity u_b throughout the recompression region. C_e is the Crocco number of the adjacent freestream which is related to the Mach number M_e by

$$C_e^2=\frac{M_e^2}{[2/(\gamma-1)]+M_e^2} \tag{6}$$

The turbulent shear stress along the dividing streamline, which appears in terms G_3 and G_4, is evaluated through an eddy diffusivity which is related to that at the initial section of recompression by

$$\frac{\epsilon}{\epsilon_m}=\frac{u_e}{u_{em}}\left(\frac{\delta_a}{\delta_{am}}\right)\left(\frac{\ell_m+x_r}{\ell_m}\right) \tag{7}$$

where δ_a refers to the shear layer thickness above the dividing streamline, and x_r refers to the distance along the recompression region. Perhaps it is worthwhile to note that with an integral analysis for the turbulent mixing and recompression process, only the empirical information of the eddy diffusivity along the dividing streamline is needed throughout these regions.

The right-hand side of Eq. (5) contains the pressure gradient term which is implicitly linked with the spread of the viscous layer into the already established inviscid flow region. Iterative solution procedures must be relied upon at each step of the numerical integration if accurate results are expected.

It was learned from the recompression calculation that by integrating the system of equations, the point of reattachment behaves as a saddle-point singularity for the system of equations describing the flow. For slightly different z_R values, which, of course, correspond to different inviscid flowfields, the dividing streamline velocity would either decrease to negative values during recompression, before the point of reattachment on the centerline of the wake is reached, or eventually break away from the trend of continuous reduction and start to increase. In the actual calculation, since the establishment of the inviscid flowfield is time consuming, the value of z_R was kept fixed, and the saddle-point behavior is observed from the fact that slightly different initial boundary-layer thicknesses before mixing would lead to widely different results toward the end of recompression. Figure 4 shows a typcial set of results of calculations showing the different trends of the normalized dividing streamline velocity, ϕ_d. To keep the computational effort within a reasonable level, one must attempt to reach the point of reattachment through extrapolation at the end of recompression when the initial boundary-layer thicknesses of two divergent trends are within a small margin.

Redevelopment of Flow

At the point of reattachment, the velocity profile has the shape of $\phi=3\zeta^2-2\zeta^3$ according to Eq. (4a). It is now assumed that throughout the region of redevelopment, the velocity has the profile

$$\phi=\phi_w+(1-\phi_w)(3\zeta^2-2\zeta^3) \tag{8}$$

where ϕ_w is the centerline wake velocity and $\zeta=r/\delta_e$. δ_e is the thickness of the viscous layer within the region of redevelopment.

The continuity equation and the equation of motion under the boundary-layer formulation are

$$\frac{\partial(\rho ur)}{\partial z}+\frac{\partial(\rho vr)}{\partial r}=0 \tag{9a}$$

$$\frac{\partial(\rho u^2 r)}{\partial z}+\frac{\partial(\rho uvr)}{\partial r}=-r\frac{dp}{dz}+\frac{\partial(\tau r)}{\partial r} \tag{9b}$$

Upon integrating across the viscous layer, Eqs. (9) readily yield

$$[1-2(1-C_e^2)I_1]\frac{d\delta_e}{dz}-(1-C_e^2)\delta_e I_4\frac{d\phi_w}{dz}$$
$$=\tan\beta_e+\left[\frac{\delta_e I}{C_e}\left(1-C_e^2\frac{3\gamma-1}{\gamma-1}\right)+2C_e\delta_e I_3(1-C_e^2)\right]\frac{dC_e}{dz} \tag{10a}$$

$$\frac{2I_2(1-C_e^2)}{\delta_e}\frac{d\delta_e}{dz}+(1-C_e^2)I_6\frac{d\phi_w}{dz}$$
$$=-\frac{dC_e}{dz}\left[\frac{2I_2}{c_e}\left(1-C_e^2\frac{2\gamma-1}{\gamma-1}\right)+2C_e(1-C_e^2)I_5\right.$$
$$\left.+\frac{1}{2C_e}(1-2(1-C_e^2)I_1)\right] \tag{10b}$$

where

$$I_1=\int_0^1\frac{\phi\zeta d\zeta}{1-C_e^2\phi^2},\qquad I_2=\int_0^1\frac{\phi(1-\phi)\zeta d\zeta}{1-C_e^2\phi^2}$$

$$I_3=\int_0^1\frac{\phi^3\zeta d\zeta}{(1-C_e^2\phi^2)^2},\qquad I_4=\int_0^1\frac{1+C_e^2\phi^2}{(1-C_e^2\phi^2)^2}\Gamma\zeta d\zeta$$

$$I_5=\int_0^1\frac{\phi^3(1-\phi)\zeta d\zeta}{(1-C_e^2\phi^2)^2},\qquad I_6=\int_0^1\frac{1-2\phi+C_e^2\phi^2}{(1-C_e^2\phi^2)}\Gamma\zeta d\zeta$$

$$\Gamma=\frac{\partial\phi}{\partial\phi_w}=1-3\zeta^2+2\zeta^3 \tag{11}$$

β_e is the streamline angle at the edge of the shear layer and all integrals, I_1 through I_6, are only functions of C_e and ϕ_w. It is to be noted that this integral analysis is equally valid for laminar or turbulent flows since the shear stress vanishes at both limits of integration. Indeed, the far-wake condition of

$$\delta_e(1-\phi_w)^{1/2}=\text{const} \tag{12}$$

is satisfied by either laminar or turbulent flow. It may be shown that the system of equations given by Eqs. (10) with the assumed velocity profile is compatible with this condition.

It has been learned from this approach of the problem that the fully developed flow condition also presents itself as a saddle-point singularity of the system of equations describing the flow. For a fixed Z_R but with slightly different δ^*_{asy} values, the redevelopment flow after the reattachment (after the point of reattachment has been obtained from extrapolation) will lead either to positive and ever increasingly large $d\delta_e/dz$ or to a smaller and eventually negative $d\delta_e/dz$ value. Negative $d\delta_e/dz$ also invariably leads to negative $d\phi_w/dz$, resulting in a reduction of wake centerline velocity. An example illustrating this phenomenon is shown in Fig. 5. Both of these behaviors are physically unrealistic and the correct value of δ^*_{asy} lies in between. This, of course, is the typical behavior of a saddle point.

It is now worthwhile to note that with Z_R and δ^*_{asy} as the characteristic parameters needed to establish the correspond-

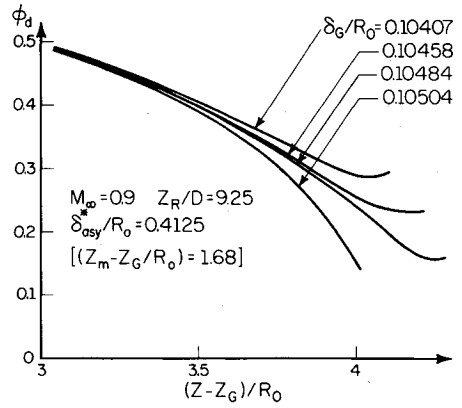

Fig. 4 Saddle-point behavior or recompression process.

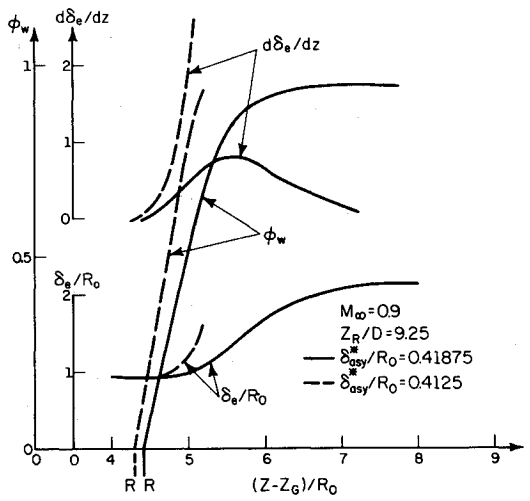

Fig. 5 Saddle-point behavior of redevelopment process.

ing inviscid flow, two saddle-point singularities provide two discriminating criteria for the determination of their correct values under the given flow conditions. However, two saddle points in sequence are mathematically "unstable," especially when the first saddle point can only be determined from extrapolation. Numerical consistency for systems of nonlinear ordinary differential equations cannot be achieved easily. For the present problem, the numerical error generated from the finite difference computation of the potential equation may also have important influences on this phase of the computations. Fortunately, an analysis of the asymptotic wake flow would relate δ^*_{asy} to the total drag experienced by the projectile, and the integration against two-saddle-point singularities in sequence is conveniently avoided.

Asymptotic Wake Flow Condition

It is stipulated that under the asymptotic far-wake flow situation, the approaching freestream external flow condition is restored. The velocity profile within the wake still obeys Eq. (8), but with $(1-\phi_w)$ as a small quantity, so that higher orders of this quantity can be ignored. According to the definition of the displacement thickness given by

$$\rho_\infty u_\infty (\delta_e^2 - \delta_{asy}^{*2}) = 2\int_0^{\delta_e} \rho u r dr \tag{13}$$

and the drag-momentum relationship for the far-wake flow given by

$$D_t = 2\pi \int_0^{\delta_e} \rho u (u_\infty - u) r dr \tag{14}$$

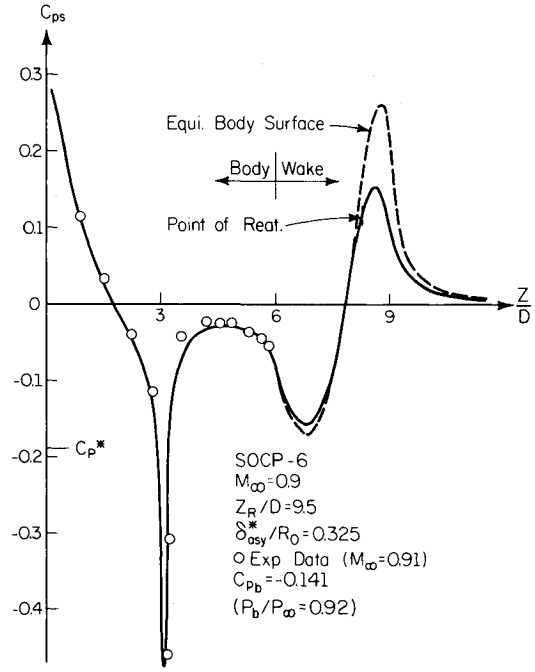

Fig. 6 Pressure distribution realized from detailed evaluations.

where D_t is the total drag experienced by the projectile, it may be shown from Eqs. (13) and (14) that

$$\left(\frac{\delta^*_{asy}}{R_0}\right) = \left[\frac{C_{Dt}}{2}\frac{1+C_\infty^2}{1-C_\infty^2}\right]^{1/2} \tag{15}$$

where

$$C_{Dt} = D_t \Big/ \frac{\rho_\infty V_\infty^2}{2}\pi R_0^2$$

The total drag D_t is the sum of the form drag, skin friction drag on the forebody,and the base drag on the base.

Method of Calculations and Results

With the introduction of the relationship given by Eq. (15), calculation procedures become greatly simplified. For a given freestream Mach number M_∞, a pair of values of z_R/D and δ^*_{asy}/R_0 is selected. The potential flow solution for this geometric configuration is established subsequently. After the turbulent jet mixing process behind the base has been analyzed, the total drag coefficient can be evaluated, and δ^*_{asy}/R_0 is immediately adjusted according to Eq. (15). Since the effect of δ^*_{asy}/R_0 on the total drag is minor, the correct value of δ^*_{asy}/R_0 can be determined usually within three iterations. Once this condition is satisfied, viscous recompression can be determined by integrating the system of Eq. (5). The dimensionless dividing streamline velocity will either be reduced to a negative value before the centerline is reached or will break away from the continuous pattern of reduction and start to increase—the saddle-point behavior. This phenomenon demands the adjustment of the z_R/D value accordingly. Once this adjustment is within a small margin ($\Delta z_R/D \leq 0.0025$ for the present series of calculations), the solution is reached even if the detailed wake flow pattern has not yet been satisfactorily established. It is entirely possible to continue these detailed calculations including the redevelopment after reattachment. Early results obtained from such efforts[27] are shown in Figs. 6 and 7 where the realized pressure field, the reproduced equivalent body, and the path of the dividing streamline are shown. The reproduced equivalent body was obtained by adding the displacement thickness of the viscous layer above the dividing streamline

onto the path of the dividing streamline. However, all of these calculations are not necessary if only the information on base and total drag is desired. Calculations have been carried out for all of the transonic Mach numbers where wind tunnel pressure data on this projectile are available.[28] The unit Reynolds number employed was also compatible with the wind tunnel test condition ($Rey/\text{ft} = 4 \times 10^6$). Figure 8 shows the pressure distribution on the equivalent body along with the experimental data on the forebody. The corresponding average base pressure coefficient and the base pressure ratio are also labeled in the figures. Under some subsonic Mach number conditions, the agreement of pressure with the data on the cylinder is less desirable although it has no influence on the forebody form drag evaluation. The base pressure ratio obtained from this study is shown in Fig. 9. Various drag coefficients and the total drag coefficient for the transonic Mach numbers are presented in Fig. 10.

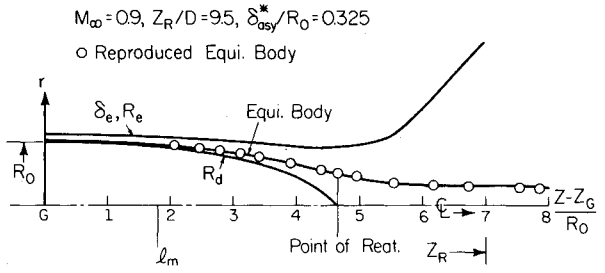

Fig. 7 Dividing streamline, viscous wake, and reproduced equivalent body.

Discussion

It should be noted that the method developed for this study should also be applicable for smaller freestream subsonic Mach number flows, including the incompressible flow condition and also for larger supersonic freestream Mach numbers. Computations of these cases have been carried out and the results are also reported in Figs. 9 and 10. Although the correctness of the base pressure ratio for $M_\infty > 1.3$ is doubtful since entropy increases from shocks may no longer be negligible, previous results of $p_b/p_\infty = 0.7625$ at $M_\infty = 1.5$ on supersonic flow past an axisymmetric backward-facing step[20] with comparable initial boundary-layer thickness seems to imply that these results are not completely unreasonable.

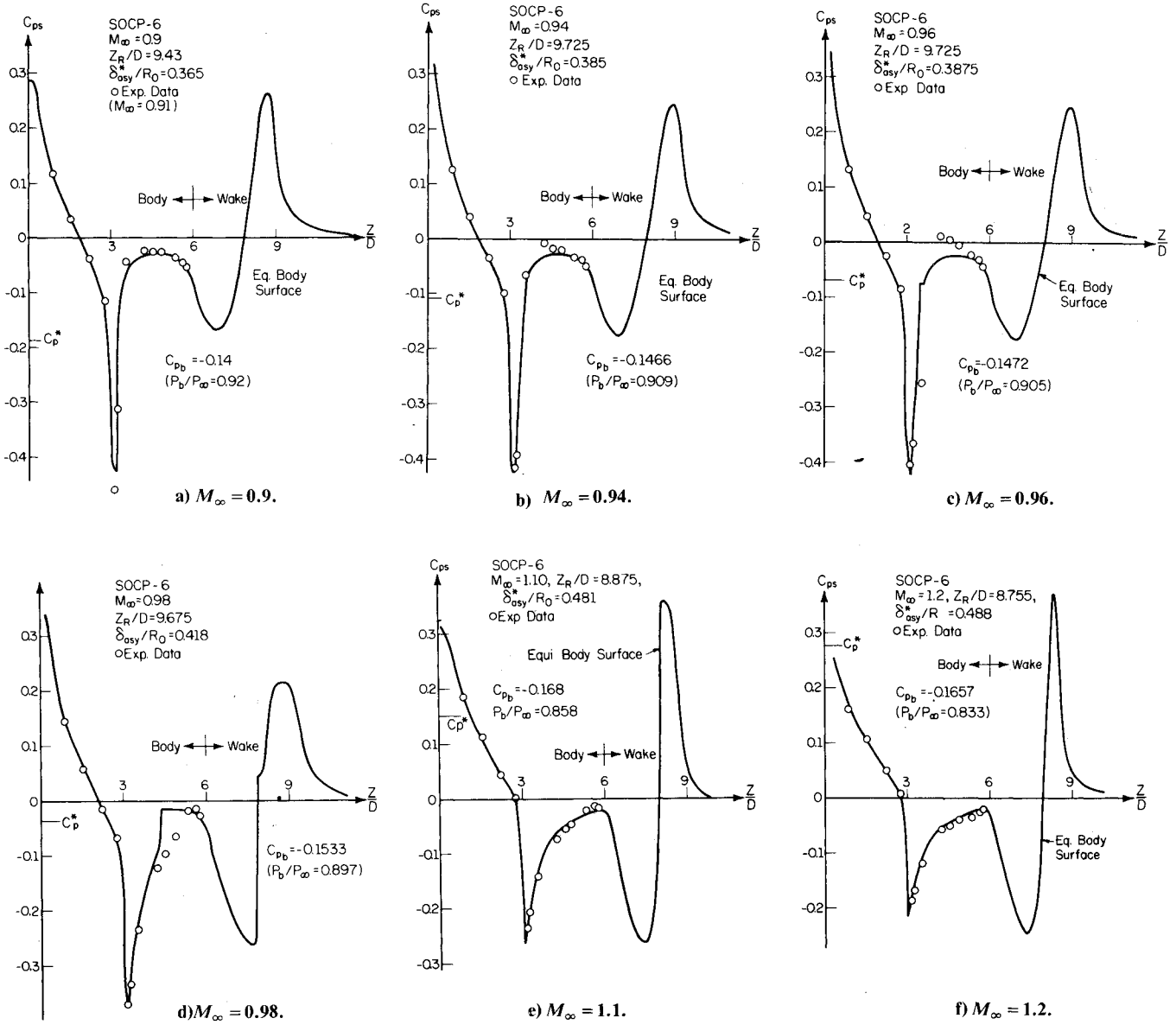

Fig. 8 Pressure distribution on an equivalent body.

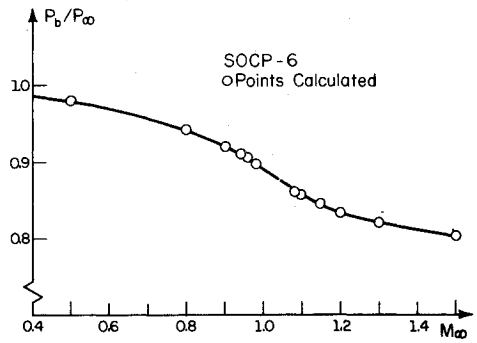

Fig. 9 Average base pressure within the transonic regime.

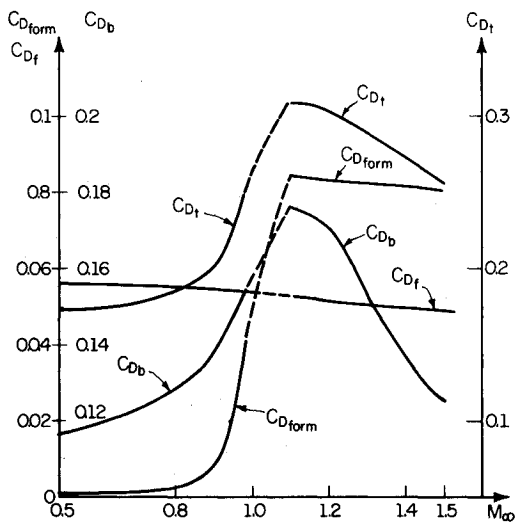

Fig. 10 Drag coefficients within transonic regime.

No computations have been carried out for the range of $0.98 < M_\infty < 1.08$. In fact, additional underrelaxation has been applied for the potential flow calculations at $M_\infty = 0.98$. Also, the calculations for the potential flow have been modified from the original scheme[25] for the supersonic approaching flows. Although it appears from Figs. 9 and 10 that base pressure results are more or less bracketed, the forebody form drag may have a peak within the range of $0.98 < M_\infty < 1.08$. Also, it is by no means a simple matter to carry out these calculations. At the least, additional underrelaxation is needed to obtain a convergent solution for the potential flow within this range of the Mach number. A considerably greater amount of computer time is also needed for these occasions.

It is obvious from this scheme of computations that the overall pressure field is produced from the characteristic parameters z_R and δ^*_{asy}. While δ^*_{asy} is directly related to the total drag experienced by the body, z_R is determined from the recompression of the free turbulent shear layer which is nevertheless guided by the already established inviscid flow. The flow mechanisms of viscid and inviscid flows are so interwoven that they all play important roles in the establishment of the solution. With an integral analysis of the viscous flows, the important flow features are brought forth clearly so that influences of different flow components and flow mechanisms can be easily identified and appreciated.

For the analysis of turbulent jet mixing process, only the empirical eddy diffusivity along the dividing streamline needs to be specified. In addition, the eddy diffusivity for the subsequent recompression process is also estimated on a similar basis. It is well known that the expression given by Eq. (2b) is valid only for constant-pressure fully developed turbulent mixing flows. In fact, the value of σ is 12 for incompressible flow, and its value tends to increase slightly with the Mach number. Perhaps more accurate evaluation of this mxing process can be obained from the two-equation turbulence modeling. It is believed, however, that the present simplified scheme will yield a fairly reasonable estimation of this process of turbulent transport. A more precise estimation can be included into the analysis in the future if it is proved necessary.

The computing time required for a complete calculation of the case of $M_\infty = 0.9$ is around 5 min on the Cyber 175 computer system. The required memory space in 21K for the computing program and 71K for its execution.

Extension to Flows with Small Angles of Incidence

The study carried out thus far is for axisymmetric configurations; thereby the flow must be at the condition of zero angle of attack.

When the angle of attack is not zero, the flow problems become three-dimensional. Even under the situation of a small angle of attack, the flow condition is so complicated that an accurate study can be based only on large-scale three-dimensional computations. Since the present analysis was based on an equivalent body concept, one may assume that the effect of the small angle of attack to the viscous flow processes is small under this situation. Essentially, it is to stipulate that the angle of attack will exert its influence only on the equivalent inviscid body which is already established for the case of zero angle of attack. It is hoped that an inviscid study of the flow past this equivalent body[30] under a small angle of incidence would yield a crude estimation of the base pressure for these flow conditions. The merit of such a speculation can be evaluated only when experimental data of this nature become abundantly available.

Acknowledgments

This work was carried out under partial support from the U.S. Army Research Office through Contract DAAG29-83-K-0043. This effort was actually initiated while the author served as a Senior Research Associate of the National Research Council, National Academy of Science, working in the Aerodynamic Research Branch, Launch and Flight Division of the U.S. Army Ballistic Research Laboratory. Valuable discussions and help from Dr. W. B. Sturek and his group in BRL are greatly appreciated.

References

[1] Crocco, L. and Lees, L., "A Mixing Theory for the Interaction Between Dissipative Flows and Nearly Isentropic Streams," *Journal of the Aeronautical Sciences*, Vol. 19, Oct. 1952, pp. 649-676.

[2] Korst, H. H., "A Theory for Base Pressures in Transonic and Supersonic Flow," *Journal of Applied Mechanics*, Vol. 22, Dec. 1956, pp. 593-600.

[3] Korst, H. H., Page, R. H., and Childs, M. E., "A Theory for Base Pressures in Transonic and Supersonic Flows," University of Illinois, Urbana, Ill., ME-TN-392-2, March 1955.

[4] Beheim, M. A., Klann, J. L., and Yeager, R. A., "Jet Effects on Annular Base Pressure and Temperature in a Supersonic Stream," NASA TR R-125, 1962.

[5] Carriere, P. and Sirieix, M., "Resultants Recent Dans L'Etude Des Problems De Melange Et De Recollement," ONERA TP 165, 1964.

[6] Korst, H. H., Chow, W. L., and Zumwalt, G. W., "Reseach on Transonic and Supersonic Flow of a Real Fluid at Abrupt Increases in Cross Section," Engineering Experiment Station, University of Illinois, Urbana, Ill., ME Tech. Rept. 392-5, Dec. 1959.

[7] Lees, L. and Reeves, B. L., "Supersonic Separated and Reattaching Laminar Flows: I. General Theory and Application to Adiabatic Boundary-Layer/Shock-Wave Interactions," *AIAA Journal*, Vol. 2, Nov. 1964, pp. 1907-1920.

[8] McDonald, H., "The Turbulent Supersonic Base Pressure Problem: A Comparison Between a Theory and Some Experimental Evidence," *The Aeronautical Quarterly*, Vol. 17, May 1966, pp. 105-126.

[9] Weinbaum, S., "Rapid Expansion of a Supersonic Boundary Layer and Its Application to the Near Wake," *AIAA Journal*, Vol. 4, Feb. 1966, pp. 217-226.

[10] Chow, W. L., "On the Base Pressure Resulting from the Interaction of a Supersonic External Stream with a Sonic or Subsonic Jet," *Journal of the Aerospace Sciences*, Vol. 26, March 1959, pp. 176-180.

[11] Page, R. H., "A Review of Component Analysis of Base Pressure for Supersonic Turbulent Flow," *Proceedings of the 10th International Symposium on Space Technology and Science*, Tokyo, Japan, 1973, pp. 459-469.

[12] Alber, I. E. and Lees, L., "Integral Theory for Supersonic Turbulent Base Flows," *AIAA Journal*, Vol. 6, July 1968, pp. 1343-1351.

[13] Addy, A. L., Korst, H. H., White, R. A., and Walker, B. J., "A Study of Flow Separation in the Base Region and Its Effects During Powered Flight," AGARD Conference on Aerodynamic Drag, AGARD-CPP-124, April 1973.

[14] Chow, W. L., "Recompression of a Two-Dimensional Supersonic Turbulent Free Shear Layer," *Developments in Mechanics, Proceedings of the 12th Midwestern Mechanics Conference*, Vol. 6, Aug. 1971, pp. 319-332.

[15] Chow, W. L. and Spring, D. J., "Viscous Interaction of Flow Redevelopment after Flow Reattachment with Supersonic External Streams," *AIAA Journal*, Vol. 13, Dec. 1975, pp. 1576-1584.

[16] Weng, C. H. and Chow, W. L., "Axisymmetric Supersonic Turbulent Base Pressures," *AIAA Journal*, Vol. 16, June 1978, pp. 553-554.

[17] Chow, W. L. and Spring, D. J., "Viscid-Inviscid Interaction of Two-Dimensional Incompressible Separated Flows," *Journal of Applied Mechanics*, Vol. 43, Ser. E, No. 3, Sept. 1976, pp. 387-395.

[18] Warpinski, N. R. and Chow, W. L., "Base Pressure Associated with Incompressible Flow Past Wedges at High Reynolds Numbers," *Journal of Applied Mechanics*, Vol. 46, No. 3, Sept. 1979, pp. 483-492.

[19] Warpinski, N. R. and Chow, W. L., "Viscid-Inviscid Interction Associated with Incompressible Flow past Wedges at High Reynolds Numbers," Engineering Experiment Station, Department of Mechanical and Industrial Engineering, University of Illinois at Urbana-Champaign, ME-TR-395-4, UILU ENG 77-4001, Feb. 1977; also, NASA CR-135246.

[20] Chow, W. L. and Shih, T. S., "Transonic Flow Past a Backward Facing Step," *AIAA Journal*, Vol. 15, Sept. 1977, pp. 1342-1343.

[21] Liu, J.S.K. and Chow, W. L., "Base Pressures of an Axisymmetric Transonic Flow Past a Backward Facing Step," *AIAA Journal*, Vol. 17, April 1979, pp. 330-331.

[22] Chow, W. L. and Shih, T. S., "The Viscid-Inviscid Interaction Associated with a Two-Dimensional Transonic Flow past a Backstep," Engineering Experiment Station, Department of Mechanical and Industrial Engineering, University of Illinois at Urbana-Champaign, ME-TR-395-3, UILU ENG 75-4003, Final Report prepared for the Research Grant, U.S. Army DAHC04-75-G-0041, Oct. 1975.

[23] Liu, J.S.K. and Chow, W. L., "Base Pressure Problems Associated with an Axisymmetric Transonic Flow past a Backward Facing Step," Department of Mechanical and Industrial Engineering, University of Illinois at Urbana-Champaign, ME-TR-395-5, Final Report prepared for Research Grant, U.S. Army DAAG29-76-G-0199, Nov. 1977 (ADA050658).

[24] Chow, W. L. Bober, L. J., and Anderson, B. H., "Strong Interaction Associated with Transonic Flow past Boattails," *AIAA Journal*, Vol. 13, Jan. 1975, pp. 112-113.

[25] Chow, W. L., Bober, L. J., and Anderson, B. H., "Numerical Calculation of Transonic Boattail Flow," NASA TN D-7984, June 1975.

[26] Brink, D. F. and Chow, W. L., "Two-Dimension Jet Mixing with a Pressure Gradient," *Journal of Applied Mechanics*, Vol. 42, Ser. E, No. 1, March 1975, pp. 55-60.

[27] Chow, W. L., "Base Pressure of a Transonic Flow past a Projectile," *Proceedings of the Symposium on Rocket/Plume Fluid Dynamic Interactions*, Vol. 1, Base Flows, Fluid Dynamic Lab., College of Engineering, University of Texas at Austin, Rept. 83-101, April 1983.

[28] Kayser, L. D. and Whiton, F., "Surface Pressure Measurements on a Boattailed Projectile Shape at Transonic Speeds," ARBRL-MR-03161, Ballistic Research Laboratory, Aberdeen Proving Ground, Md., March 1982.

[29] Weng, C. H., "Base Pressure Problems Associated with Supersonic Axisymmetric External Flow Configurations," Ph.D. Thesis, Department of Mechanical and Industrial Engineering, University of Illinois at Urbana-Champaign, 1975.

[30] Nakayama, A. and Chow, W. L., "Calculations of Transonic Boattail Flow at a Small Angle of Attack," Department of Mechanical and Industrial Engineering, University of Illinois at Urbana-Champaign, ME-TN-395-6, Report prepared for Research Grant NGL 14-005-140, April 1979; also, NASA CR-158471.